International Journal of Applied Earth Observation and Geoinformation 52 (2016) 221–229

Contents lists available at ScienceDirect

International Journal of Applied Earth Observation and Geoinformation

journal homepage: www.elsevier.com/locate/jag

Monitoring dam structural health from space: Insights from novel InSAR techniques and multi-parametric modeling applied to the Pertusillo dam Basilicata, Italy

Pietro Milillo[a,b,c,*], Daniele Perissin[d], Jacqueline T. Salzer[e], Paul Lundgren[c], Giusy Lacava[a], Giovanni Milillo[f], Carmine Serio[a]

[a] Scuola di Ingegneria, Universita' Degli Studi Della Basilicata, Potenza, Italy
[b] Seismological Laboratory, California Institute of Technology, Pasadena, CA, USA
[c] NASA, Jet Propulsion Laboratory, Pasadena, CA, USA
[d] School of Civil Engineering, Purdue University, West Lafayette, IN, USA
[e] Department 2: Physics of the Earth, GFZ German Research Centre for Geosciences, Potsdam, Germany
[f] ASI Italian Space Agency, Matera, Italy

ARTICLE INFO

Article history:
Received 2 February 2016
Received in revised form 8 June 2016
Accepted 11 June 2016

Keywords:
Time-series analysis
Dam
HST and HTT model
SAR
Interferometry

ABSTRACT

The availability of new constellations of synthetic aperture radar (SAR) sensors is leading to important advances in infrastructure monitoring. These constellations offer the advantage of reduced revisit times, providing low-latency data that enable analysis that can identify infrastructure instability and dynamic deformation processes.

In this paper we use COSMO-SkyMed (CSK) and TerraSAR-X (TSX) data to monitor seasonal induced deformation at the Pertusillo dam (Basilicata, Italy) using multi-temporal SAR data analysis. We analyzed 198 images spanning 2010–2015 using a coherent and incoherent PS approach to merge COSMO-SkyMed adjacent tracks and TerraSAR-X acquisitions, respectively. We used hydrostatic-seasonal-temporal (HST) and hydrostatic-temperature-temporal (HTT) models to interpret the non-linear deformation at the dam wall using ground measurements together with SAR time-series analysis. Different look geometries allowed us to characterize the horizontal deformation field typically observed at dams. Within the limits of our models and the SAR acquisition sampling we found that most of the deformation at the Pertusillo dam can be explained by taking into account only thermal seasonal dilation and hydrostatic pressure. The different models show slightly different results when interpreting the aging term at the dam wall. The results highlight how short-revisit SAR satellites in combination with models widely used in the literature for interpreting pendulum and GPS data can be used for supporting structural health monitoring and provide valuable information to ground users directly involved in field measurements.

© 2016 Elsevier B.V. All rights reserved.

1. Introduction

Dams are anthropogenic barriers that provide a series of advantages for human activities such as water and/or electricity supply and flood protection. However, water impoundment by means of a dam leads to safety concerns related to induced embankment breaks or overtopping.

Earthquakes, landslides, erosion and aging are among the causes of dam failure and subsequent uncontrolled water release. Several instruments and procedures have been developed for monitoring and predicting dam behavior and mitigating the socio-economical risk. Most of them take into account ground based measurements using GPS or pendulum displacements (Chouinardet al., 1995; Behr et al., 1998; De Sortis and Paoliani, 2007; Lombardi et al., 2008; Amberg, 2009; Ehiorobo and Irughe-Ehigiator, 2011; Li and Wang, 2011; Barzaghi et al., 2012). A discrete number of studies have been conducted during the past 15 years for structural health monitoring of dams using SAR data (Tarchi et al., 1999; Blom et al., 1999; Wang et al., 2010; Arjona et al., 2010; Grenerczy and Wegmüller, 2011; Vöge et al., 2011; Tomás et al., 2013; Di Martire et al., 2014; Michoud et al., 2015a,b; De Sousa et al., 2015; Roque et al., 2015; Mazzanti et al., 2015).

* Corresponding author at: Scuola di Ingegneria, Universita' Degli Studi Della Basilicata, Potenza, Italy.
E-mail addresses: pietro.milillo@unibas.it, pietro0milillo@gmail.com (P. Milillo).

http://dx.doi.org/10.1016/j.jag.2016.06.013
0303-2434/© 2016 Elsevier B.V. All rights reserved.

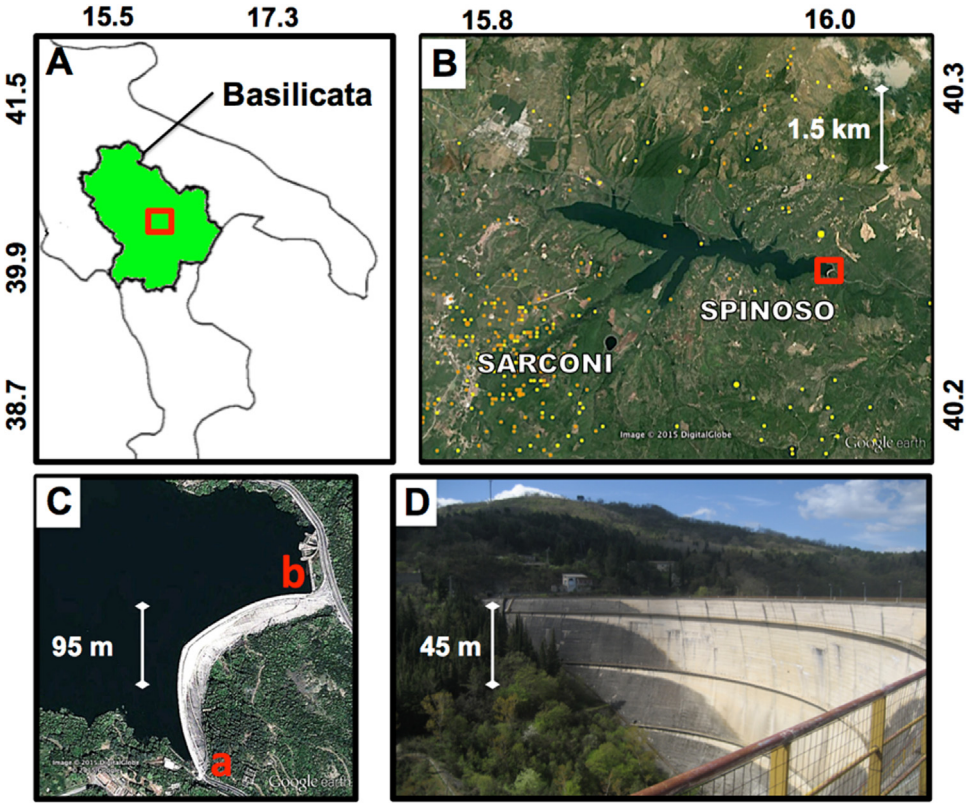

Fig. 1. Overview of the study site (A) South Italian Peninsula; the red outline shows the extent of the Pertusillo artificial lake in B. (B) Google-Earth Optical Image showing the "Lago di Pietra del Pertusillo". Seismicity at the Pertusillo dam recorded by the ISIDE-INGV network. Yellow (orange) dots indicates earthquakes with 0–10 (10–20) km depth The red box shows the extent of the dam in C. (C) Google-Earth optical image evidencing the sides of the dam(D) side view of the dam. Scale bar is referenced to the height of the dam. (For interpretation of the references to colour in this figure legend, the reader is referred to the web version of this article.).

Only recently have analyses been conducted to investigate the achievable accuracy and sensitivity of SAR displacement measurements at dams (Wang et al., 2010; Di Martire et al., 2014). The surge in available high quality InSAR data coming from international constellations of SAR satellites are transforming InSAR based time-series analysis techniques into near-real-time operational tools able to deliver useful information to ground users (Milillo et al., 2015; Riel et al., 2015; Lundgren et al., 2015) providing an increased sensitivity to displacements that highlights the dynamic behavior of natural and anthropogenic phenomena. In this paper we use a multi-temporal InSAR technique to examine non-linear displacements at the Pertusillo dam (Basilicata, Italy), combining coherent CSK parallel tracks with incoherent TSX and CSK X-band data (3 cm wavelength). This technique, initially applied with ERS, ENVISAT and ALOS SAR datasets (Perissin et al., 2007a,b; Perissin, 2008; Perissin and Prati, 2008) allowed us to decrease the acquisition repeat time down to 8 days on average, with sporadic same day acquisitions from CSK and TSX. The TSX and CSK time-series were compared to ALOS L-band data (24 cm wavelength) spanning a different time period, underlining the fundamental role of the finer temporal and spatial resolution in illuminating new aspects of the deformation dynamics of a dam. We used ascending and descending tracks to constrain vertical and horizontal movements and characterize horizontal displacements at the dam crown. The time-series analysis drives hydrological-season-time (HST) and hydrological-temperature-time (HTT) models for interpreting displacements at the dam (Léger and Leclerc, 2007). These models include ground-based data such as water levels, water elevation at the dam wall and temperature records. The two models interpret most of the deformation in terms of seasonal temperature oscillations and hydrostatic pressure at the dam walls. We find slightly different results when interpreting linear temporal deformation trends and provide a possible explanation. We explain this difference as the effect of the non-uniform temporal acquisition sampling and the temperature records included in the HTT model.

The paper is organized as follows. First, the Pertusillo reservoir is described. Then a brief description of the dataset is given followed by a brief summary of the basic concepts of InSAR and multi-temporal InSAR technique, coherent/uncoherent data merging and a description of interpretative models for concrete dams. Finally, the deformation fields obtained with the PS technique are used to constrain HST and HTT models. The result shows how very short repeat time interferometry is leading to unprecedented observational capabilities able to efficiently characterize the dynamic behavior of a dam.

2. Test site

2.1. Geological setting

The Pertusillo Dam is located in the southern part of the Agri Valley (Val d'Agri in Italian) and is mainly used for producing hydroelectric energy and irrigation of the Puglia and Basilicata regions. The Val d'Agri is a Quaternary intermountain fault-bounded basin in the Lucanian Appennines (Fig. 1). The area is characterized by a high seismogenic potential as testified by the occurrence of destructive earthquakes, (such as the 1857 Mw 7 Basilicata Earthquake and the 1980 Mw 6.9 Irpinia earthquake, Giocoli et al., 2014). Induced seismicity by recharge of the Pertusillo reservoir and fluid reinjection had also been recorded recently (Stabile et al., 2014a,b; Giocoli 2014) suggesting a one dimensional pore fluid pressure diffusion physical mechanism involving the Northeast-Southwest

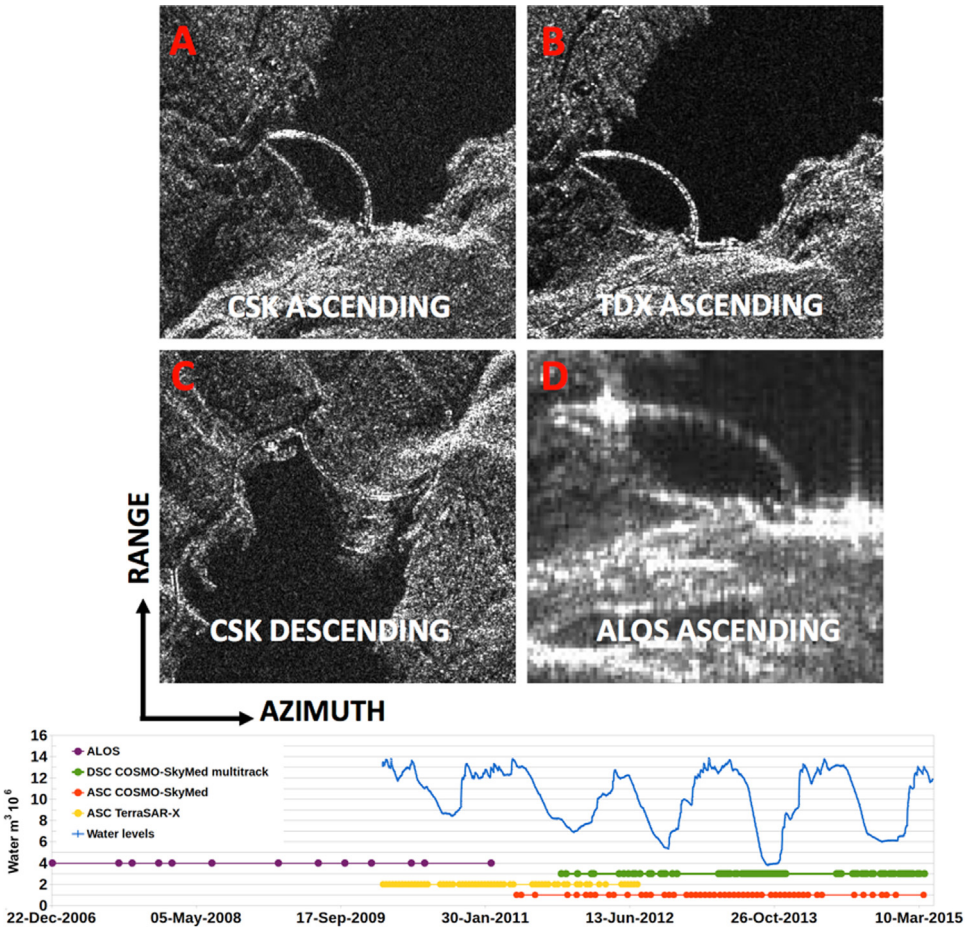

Fig. 2. Mean amplitude images over the Pertusillo dam (A) CSK ascending (B) TSX ascending (C) CSK descending (D) ALOS ascending. The plot on the bottom shows the temporal distribution of each dataset, red CSK ascending, yellow TDX ascending, green CSK multi-track descending and blue water levels at the Pertusillo dam during the acquisition time span. Water level data are not available before 2009. (For interpretation of the references to colour in this figure legend, the reader is referred to the web version of this article.)

fault zones connecting the reservoir to the Monti della Maddalena fault system (Stabile et al., 2014a,b).

The 98 m high 357 m long arch-gravity dam impounds water coming from the Agri river collected in the "Lago di Pietra del Pertusillo", an artificial lake built between 1957 and 1962. The basin capacity amounts to 155 10^6 m^3. On December 28th 2014 an Mw 3.2 earthquake occurred, the epicenter being located at a distance of about 1 km and a depth of 16.5 km from the dam. Official reports do not classify this event as induced seismicity due to fluid reinjection and water recharge of the Pertusillo basin (ENI Report, 2014). Our results do not show any significant deformation occurring at the dam related to this event.

2.2. Dataset

We analyzed five interferometric datasets, three from ascending and two from descending tracks. We processed a total of 201 SAR scenes that are divided among three COSMO-SkyMed tracks: one ascending (Fig. 2A) and two adjacent descending (Fig. 2C), each with a right-looking radar direction and incidence angles of 30° for the ascending (satellite moving North and looking East) and 29 and 30° for the descending (satellite moving South and looking West) geometries spanning 2010–2015. For TerraSAR-X we use an ascending track, right looking SAR with incidence angle 39° covering the years 2010–2012 (Fig. 2B). For ALOS we use an ascending track, right looking SAR, with incidence angle 34° covering the years 2006–2010 (Fig. 2D). Polarization is HH (horizontal transmit and receive). Table I in the supplementary material shows the datasets used for our analysis. The acquisitions were planned to facilitate short-repeat time interferometry, avoiding holes in the acquisition plan. The COSMO-SkyMed dataset is based on the MapItaly project covering the entire Italian Peninsula. The ascending dataset is composed of a dense and uniform acquisition plan, while the descending tracks suffered frequent interruptions during the period December-April 2012–2014. The TerraSAR-X datset is the densest (11 days repeat time) compared to COSMO-SkyMed (only one CSK satellite acquired data at the 16 day repeat time according to the MapItaly acquisition plan). The ALOS sensor acquired only 14 images over a period of six years. Due to the dam lying near the center of the CSK ascending track we were not able to image it from adjacent overlapping ascending tracks.

Ascending and descending geometries observes the dam with different incidence and heading angles. A schematic description of the scattering mechanisms and sensitivity to different parts of the dam is presented in Fig. 3.

The descending data (Fig. 2C) are characterized by foreshortening showing the crown before the basement in the range direction. The ascending data (Fig. 2A) are affected by shadowing, which hides the basement of the dam. A first visual analysis of the seasonal water level changes at the dam can be performed looking at the ascending amplitude images and the different double bounce angles (Fig. 4). The descending dataset does not show this scattering effect. It is important to discuss the relative orientation of the dam to the range direction and the incidence angle of the radar. The ascend-

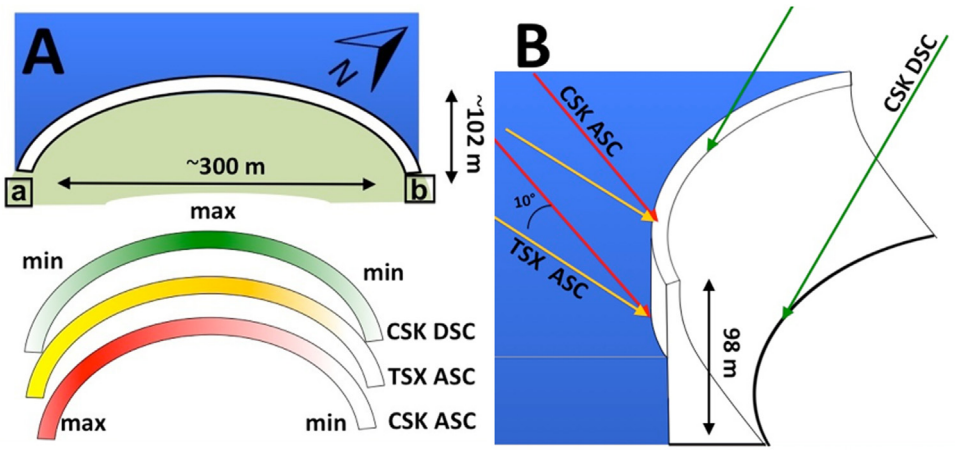

Fig. 3. Schematic representation of the Pertusillo dam as seen from the SAR satellites in terms of electromagnetic scattering and phase sensitivity to deformation. (A) Different tracks sensitivity to horizontal displacements perpendicular to the dam wall (B) Shadowing and foreshortening scattering mechanism characterizing the dam wall. ALOS has not been represented since it follows the TSX and CSK ascending sensitivity and scattering scheme.

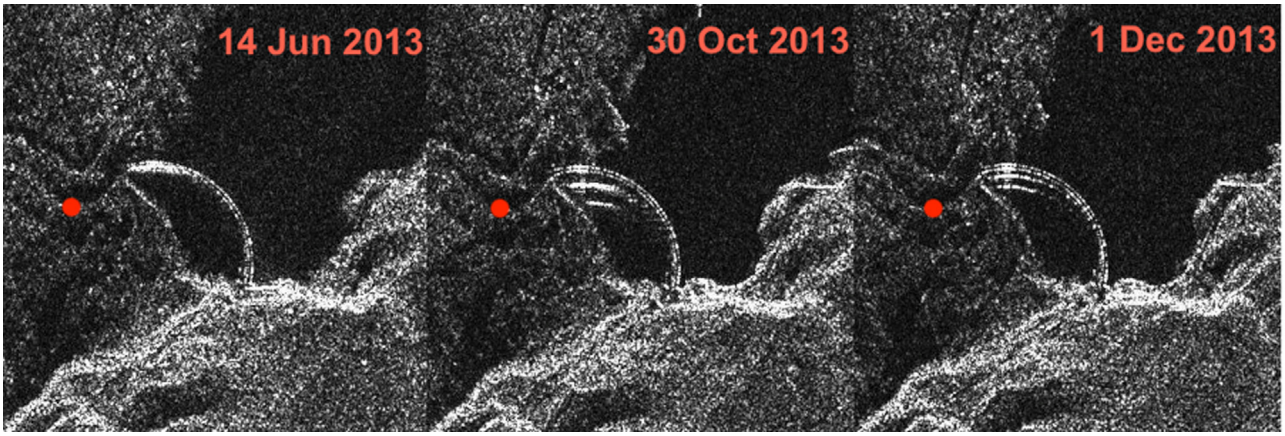

Fig. 4. Double bounce effect recorded during different periods of the year affecting the CSK ascending. The descending dataset does not show this effect. Reference point used for PS-InSAR analysis showed in red.

Table 1
LOS projection vector components for the east, north, up components of deformation.

Incidence °	Heading °	North	East	Up Sensor
30	350	0.09	0.49	0.87 CSK ASC
39	357	0.14	0.61	0.78 TSX ASC
29	190	0.08	−0.48	0.87 CSK DSC
34	352	0.08	0.55	0.83 ALOS

ing datasets are more sensitive to radial displacements of the dam at the center and South-side (Point a in Figs. 3 and 1C) while the descending datasets are more sensitive at the center of the crown decreasing their sensitivity toward the sides of the dam (Point a and Point b in Figs. 3 and 1C). Vertical displacements are independent of the relative orientation between the dam and the SAR antenna and only depend on the incidence angle. It is interesting to calculate the projection vector components for each component (Table 1).

InSAR observations are mostly sensitive to the vertical component. However, The incidence angles available for our analysis allow us to observe horizontal component of motion. A schematic description of the LOS sensitivity to horizontal and vertical displacement is shown in Fig. 3.

3. Techniques

3.1. Multi-temporal InSAR for monitoring non-linear motion

To measure time variable deformation from a single set of SAR images we use the SARPROZ software (Perissin et al., 2011) applying an extension of the standard linear PS technique (Ferretti et al., 2000, 2001) to solve for non-linear motion with no *a priori* information (Colesanti et al., 2003). The PS technique assumes a set of N + 1 co-registered SLC SAR images. We generate N single look differential interferograms with respect to a single master image. We neglect atmospheric phase screens given the small area of interest (less than 2 km^2) and adopt a stochastic model as proposed in (Ferretti et al., 2001). To do this we unwrap our PS candidates in space using the DEM error term. Once the data are unwrapped we estimate the low pass component using a 5 samples temporal baseline weighted moving average and assume this residual phase term as an estimation of the non-linear motion contribution.

3.2. Coherent and incoherent merging

We carried out multiple sensor analysis and parallel track analysis (Perissin et al., 2007a; Perissin, 2008). The main scope of these experiments was to reach a sufficient number of images for a PS-like analysis and provide temporal continuity to the time series. In

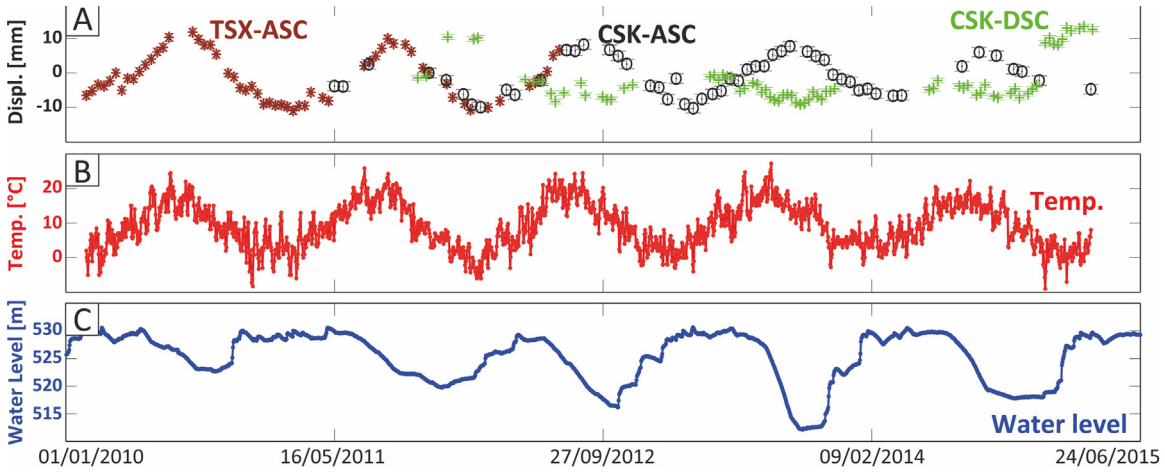

Fig. 5. (A) Cumulative displacement at the center of the dam wall. TSX ascending (cyan star), CSK descending multitrack analysis (green cross), CSK ascending (black circle). (B) Temperature records (C) water height variation at the dam wall. (For interpretation of the references to colour in this figure legend, the reader is referred to the web version of this article.)

our case we applied these methodologies in order to increase the temporal sampling and the sensitivity to thermally and hydrologically induced deformation. We merged two datasets considering separate master scenes, merging the two dataset in the geocoding stage covering a total period of 5 years (2010–2015) for a total of 112 ascending acquisitions (60 TSX, 52 CSK). Two descending tracks of 89 images were coherently merged (i.e. the data coregistered on the same stack) decreasing the average repeat time to 8 days with holes during the winter period (December–April). The CSK MapItaly acquisitions over Pertusillo lake maintained a nearly continuous incidence angle across different parallel tracks. This allowed us to coherently merge overlapping areas across the two adjacent tracks only if the location of the scatterer within the cell was very accurate. A very precise coregistration is fundamental for exploiting the parallel track interferometric phase. The main task for data combination from multiple tracks and different sensors is the identification of multi-angle targets. In our case poles and a fence are located on the crown of the dam. These targets ensure a sufficient amplitude stability (Fig. 1D). The result of the whole analysis is very sensitive to the geocoding process for which a ground control point was chosen (Fig. 4).

3.3. Time-displacement model for concrete dams

Studying how a barrier reacts to external stress is fundamental for understanding the primary phenomena responsible for crest displacement. Part of the structural health monitoring of concrete dams is based on the interpretation of displacement measurements from direct or inverse pendulums. Several statistical or deterministic models have been developed for interpreting dam deformation. Here we used the Hydrostatic-Seasonal-Time (HST) and the Hydrostatic-Temperature-Time (HTT) statistical deterministic models to interpret deformations perpendicular to the Pertusillo dam crown. These models are suitable for elastic structures and are based on the superimposition principle in which every effect sums up linearly and is weighted by a coefficient. The HTT (HST) models relate the thermal (seasonal) effect and hydrostatic loads to the structural response. In the HST model the thermal effects are modeled as the sum of an annual sinusoids while the HTT model uses a direct measurement of temperature at the dam walls. Both models assume a hydraulic load described by the water elevation as a polynomial plus linear or exponential terms, indicating irreversible strain and other unexpected behavior. Pendulum displacements can be written for each model as:

$$\delta_{HST} = a\cos\left(\frac{2\pi t}{365}\right) + b\cos\left(\frac{2\pi t}{365}\right) + cH_W + dH_W^2 + eH_W^3 + fH_W^4 + gt + h \quad (6)$$

$$\delta_{HTT} = aT + b + cH_W + dH_W^2 + eH_W^3 + fH_W^4 + gt \quad (7)$$

where δ is displacement in millimeters, t is the time in days, H_w is the water level, T is the recorded temperature and a–f are estimated using a least squares method. The HST model does not use a direct measurement of temperature and it may lack robustness when cyclic water level variations are in phase with seasonal temperature variations. This could be the case of dams used for hydroelectric production.

4. Results and discussion

We processed ALOS, TDX and CSK data with the SARProZ software (Perissin et al., 2011). The sparseness of the ALOS acquisitions and the low resolution make the interpretation of the calculated displacements difficult. The multi-temporal non-linear technique cannot be applied given the few acquisitions available over the area and a PS processing that, assuming a linear model, shows no evident deformation for the few PS identified at the dam. On the contrary the integration of CSK and TDX measurements highlights the dynamic deformation of the crown of the dam (Figs. 5–7). SAR measurements need to be analyzed together with ancillary data for interpreting the observed seasonal displacement. Hence, it is fundamental to also consider water height at the dam wall and temperature measurements.

Fig. 5 shows a time-series plot from ascending and descending TSX and CSK data with water height and temperature records for a nearby station (lat. 40.0875, lon. 16.0136). Both ascending and descending data show a periodic behavior that is the sum in phase of both temperature and water height data. The similar incidence angles between the ascending CSK and TDX dataset (7–10° difference) translates into a similar sensitivity to vertical and horizontal displacements (Fig. 3). Ascending and descending datasets have comparable seasonal amplitudes of about 10 mm and opposite phase (Fig. 6), suggesting that the deformation is purely horizontal. Moreover deformation along the dam crown is compatible with both ascending and descending LOS sensitivity to dam radial displacements (Figs. 3 A, 6 and 7). The largest displacements are located at the center of the dam crown and decrease toward the edges. This behavior has been observed at dams when interpreting

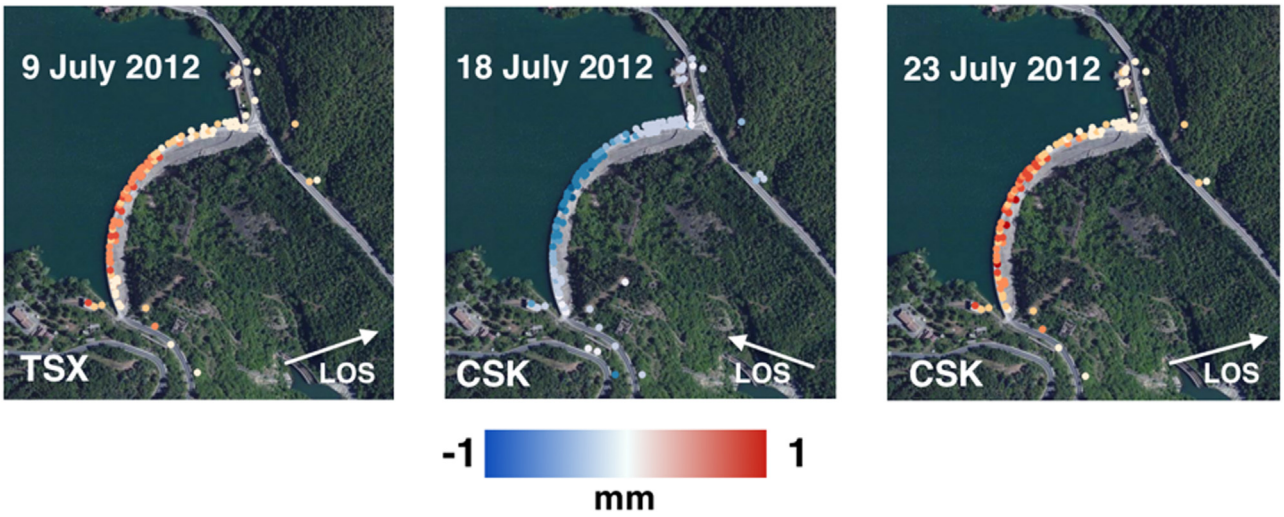

Fig. 6. Cumulative displacement maps at the Pertusillo dam as observed from different sensors and different look geometries. Negative values indicates motion away from the satellite. Optical image from Bing Maps.

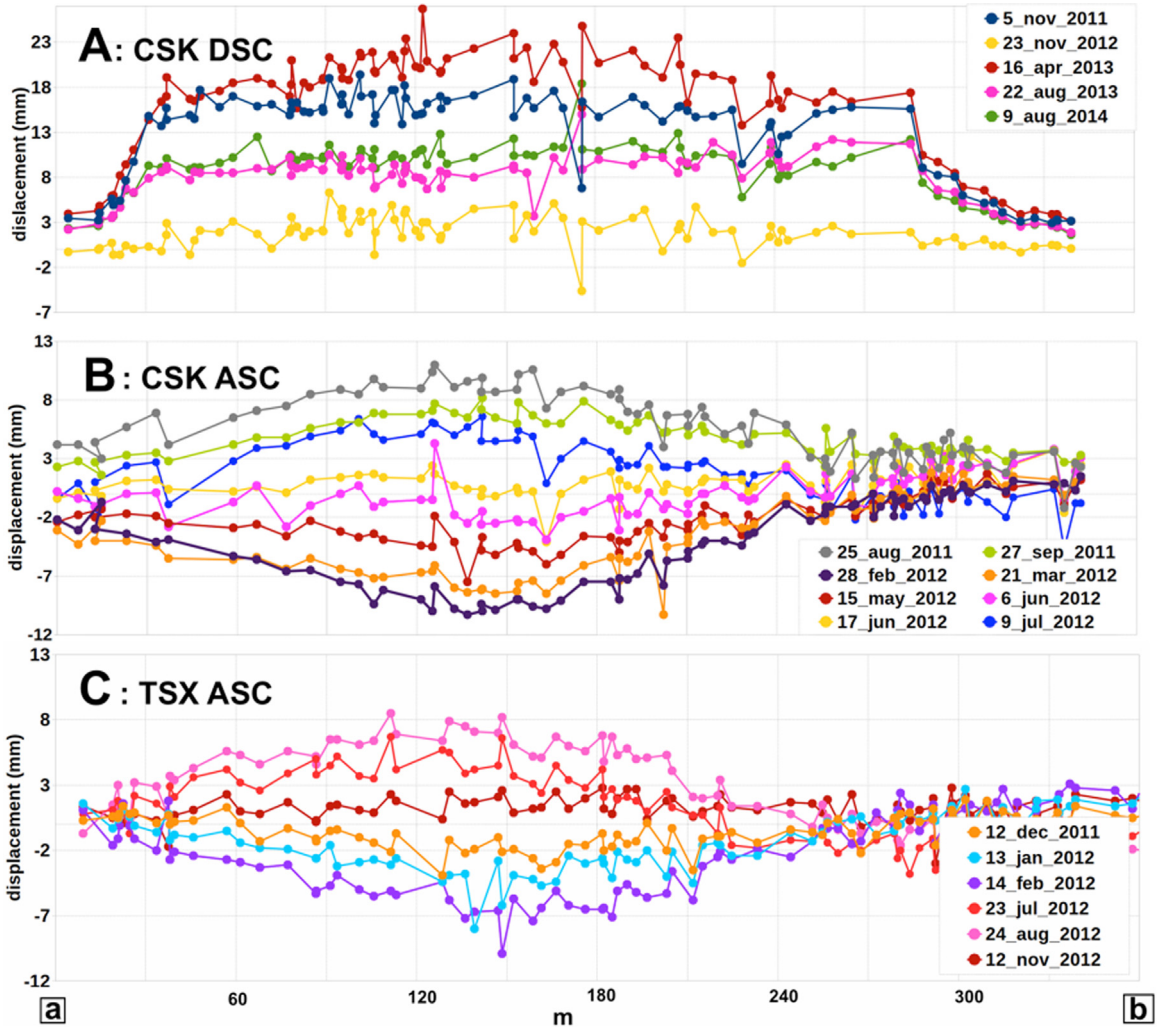

Fig. 7. Displacement profiles along the dam wall. (A) CSK descending multitrack analysis. (B) CSK ascending dataset. (C) TerraSAR-X ascending. The *a* and *b* letters refer to Figs. 1 C and 3 A. The deformation pattern is compatible with the LOS sensitivity values show in Fig. 3 and Table 1.

pendulum data that measures displacements perpendicular to the dam wall (Barzaghi et al., 2012). We generate a 2D model merging ASC and DSC data using a multi-parametric approach described in (Milillo, 2016). We used only ASC and DSC CSK data overlapping in time and estimate a thermal,-hydrological component perpendicular to the dam wall and estimate an aging term for the vertical and

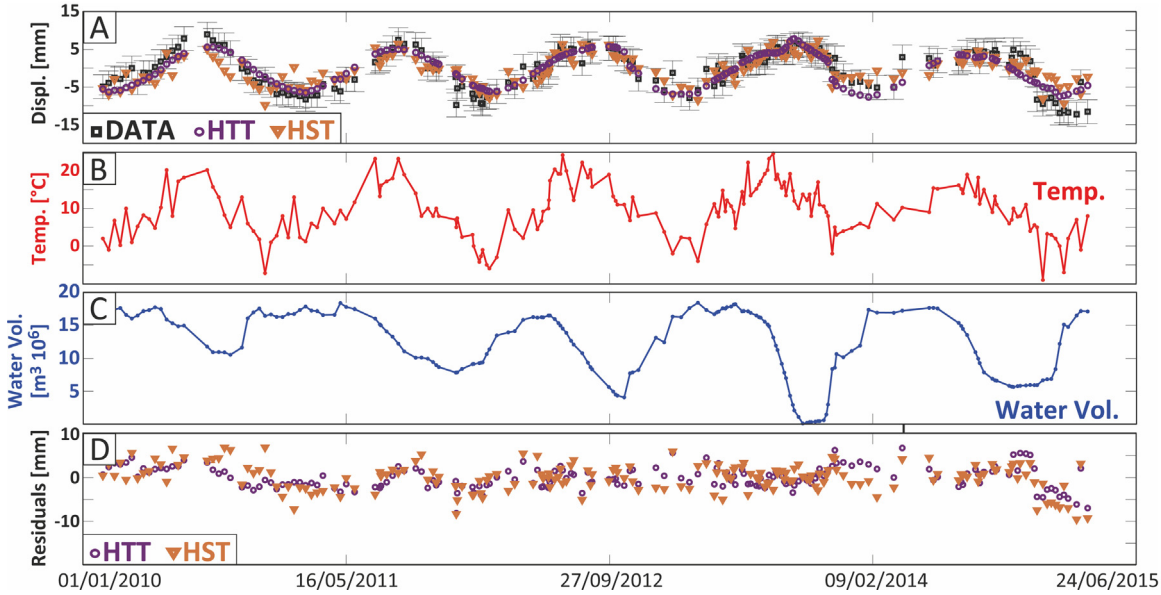

Fig. 8. (A) Projected horizontal displacement perpendicular to the dam recoded at the center of the dam. Black squares, data, magenta triangles, HTT model, green circles HST model. (B) Temperature records (C) water height variation at the dam wall. (D) residuals, magenta triangles, HTT model, green circles HST model. (For interpretation of the references to colour in this figure legend, the reader is referred to the web version of this article.)

Table 2
LOS and re-projected measurements variance for each sensor used in the time-series analysis.

$\|\gamma\|$	σ_{LOS}(mm)	$\sigma_{\perp dam}$ (mm) Sensor
0.90	1.14	2.99 CSK ASC
0.86	1.37	2.84 CSK DSC
0.96	0.7	2.94 TSX ASC

horizontal component of motion. We did not find any relevant aging term in the vertical direction occurring during the period of observation covered by CSK. In order to exploit the entire dataset we will hereby assume that the observed time-series displacements are purely horizontal radial to the dam. We can re-project the displacement in the radial direction to the dam wall.

Considering the LOS vector d_{LOS} we can write:

$$d_{\perp dam} = \frac{d_{LOS}}{\sin(\theta)\cos(\psi)} \tag{8}$$

where θ is the incidence angle and ψ is the angle between the azimuth direction (flight direction of the radar) and the direction perpendicular to the dam wall.

We can calculate the variance of our measurements after maximizing the absolute value of the temporal coherence as in (Colesanti et al., 2003):

$$\sigma_{LOS} \approx \frac{\lambda}{4\pi}\sqrt{-2ln|\gamma|} \tag{9}$$

$$\sigma_{\perp dam} = \frac{\sigma_{LOS}}{\sin(\theta)\cos(\psi)} \tag{10}$$

Table 2 shows the estimated $\sigma_{LOS}$and $\sigma_{\perp dam}$ for each dataset.

After re-projecting all three datasets into the same geometry radial to the dam walls the increased number of data samples in the dataset allows us to apply the HST and HTT statistical deterministic models. Fig. 8 shows the re-projected and modeled displacement radial to the dam wall recorded at the top center of dam and its relative residuals. The standard deviation of the residuals is below 3 mm for both the HST and the HTT models. Table 3 shows the list of the parameters obtained for both models.

Table 3
Model Parameters found with the HTT and HST models with two sigma values reported.

Coefficients (eq. 6–7)		HST	HTT
Thermal	a	-5.5 ± 0.5 mm	-0.5 ± 0.07 mm/Celsius
	b	-0.57 ± 0.1 year	
Hydrostatic	c	-14.4 ± 6	12.71 ± 7
pressure	d	-108.4 ± 140	-22.44 ± 150
	e	165.0 ± 170	-27.83 ± 160
	f	-77.54 ± 90	12.48 ± 95
Aging	g	-0.5 ± 0.22 mm/year	0.001 ± 0.003 mm/year
	h	-1000 ± 500	-1300 ± 700
R^2		0.92	0.89

One of the most important parameters is the linear term, which is not correlated with either thermal or hydrological displacements. This term is usually called the "aging term" and it is an irreversible displacement component that could be considered as an indicator of potential structural instabilities (Léger and Leclerc, 2007). The most significant difference between the two adopted interpretative models consist in the aging term. The HST model estimates a 0.5 ± 0.22 mm/year while the HTT model shows values below the significance level. Model validation is beyond the scope of this paper and may be a hard task if ground measurements (GPS or direct/reverse pendulum) are not available, as in our case. We can still make some considerations regarding the residuals and the models adopted. The HST model seems to indicate a linear irreversible deformation trend in time with smaller model residuals when compared to the HTT model. The HTT model on the other hand requires one less parameter (7 vs 8) to explain the observed deformation at the Pertusillo dam with slightly larger residuals (2.4 vs 2.9 mm). Moreover, the temperature data have been recorded 20 km away from the dam wall, which put our analysis in a non-optimal scenario for time-series interpretation using the HTT model. The temperature data and the simplicity of the models may be a limiting factor for providing a more accurate interpretation. Also the non-simultaneous ascending and descending acquisition

times make a rigorous non-parametric three-dimensional displacement decomposition not feasible.

5. Conclusions

In this work, we present a PS time-series analysis combining multiple track and multiple sensors for monitoring seasonal induced deformation. Our results show how the combination of different datasets together with the short–repeat time interferometry available with the second generation of SAR sensors can provide a valuable tool for monitoring deformation at the Pertusillo dam, and dams in general.

InSAR-based methods can be used in combination with ground surveys at the dam as well as for planning and optimizing the installation and the position of monitoring stations. The high-resolution of SAR images also allows for estimating deformation at a larger number of points compared to traditional techniques (GPS or pendulum measurements). The combination of InSAR and deterministic models for seasonally and hydrologically induced dam deformation allow interpreting deformation at the dam wall in near-real-time without the need of ground surveys. The nature of these statistical models requires a copious number of acquisitions in order to stabilize the inverted parameters as required for interpretive models with pendulum measurements. We highlight how different models may lead to different interpretations given the simple nature of the model and the elastic behavior assumption. These models have been used and validated in several studies (Chouinard et al, 1995; De Sortis and Paoliani, 2007; Amberg, 2009; Barzaghi et al., 2012) and are widely accepted within the structural engineering community. Viscosity rheology or more detailed models using finite element method models could also be adopted to provide more accurate results taking into account the inelastic behavior of the concrete.

The major limitation of this kind of analysis is the relative non-orthogonal orientation of the dam walls to the satellite flight direction. The use of high-resolution spotlight interferometry has provided useful information even in rural areas (Milillo et al., 2014) and its improved spatial resolution and phase sensitivity could partially overcome this issue. The ability of interpretative models to explain deformation measurements provided by SAR data allows us to link the InSAR remote sensing technique to the structural engineering of dams, thus providing a valuable tool supporting civil engineers and complementing ground measurement data giving a synoptic near-real time view of the dam structure health status.

Acknowledgements

We thank the Italian Space Agency (ASI) for providing COSMO-SkyMed data for this project. Original COSMO-SkyMed product ASI Agenzia Spaziale Italiana (2014–2016). We thank the German Aerospace Centre (DLR) for providing TerraSAR-X data for this project. TerraSAR-X data were provided under proposal LAN2959. ALOS PALSAR data were provided courtesy of the Japan Aerospace Exploration Agency (JAXA), Minestry of Economy, Trade and Industry (METI), which were distributed by the Earth Remote Sensing Data Analysis Center (ERSDAC). METI and JAXA retain ownership of the original ALOS PALSAR data. All the reservoir data (from 2010 to June 2011) have been provided by the Ente per lo Sviluppo dell'Irrigazione e la Trasformazione Fondiaria agency of Potenza, Italy. The seismic data can be obtained from the Istituto Nazionale di Geofisica e Vulcanologia (INGV) ISIDE database http://iside.rm.ingv.it/http://iside.rm.ingv.it/ (data available since 7 July 2015; last accessed July 2015). The work of P. Milillo was done while he was a visiting student researcher at Caltech and partially sponsored by the National Aeronautics and Space Administration Postdoctoral Program.

Appendix A. Supplementary data

Supplementary data associated with this article can be found, in the online version, at http://dx.doi.org/10.1016/j.jag.2016.06.013.

References

Amberg, F., 2009. Interpretative models for concrete dam displacements1. In Comisión Internacional de Grandes Presas-Vigésimo tercer congreso de Grandes Presas, Brasilia.

Arjona, A., Santoyo, M.A., Fernández, J., Monells, D., Prieto, J.F., Pallero, J.L.G. et al., 2010. On the applicability of an advanced DInSAR technique near Itoiz and Yesa reservoirs, Navarra, Spain. Proc. Fringe 20091609-042X Frascati: ESRIN (ESA, SP-677, 6 pp., CD).

Barzaghi, R., Pinto, L., Monaci, R., 2012. The monitoring of gravity dams: two tests in Sardinia, Italy. FIG Working Week (Session TS01F), Rome, Italy, 6–10.

Behr, J., Hudnut, K., King, N., 1998, September. Monitoring structural deformation at Pacoima dam, California using continuous GPS. In Proceedings of ion GPS, l, 11, pp. 59–68, Institute of Navigation.

Blom, R., Fielding, E., Gabriel, A., Goldstein, R., 1999. Radar interferometry for monitoring of oil fields and dams: Lost Hills, California and Aswan, Egypt. Issue Date: 25-Oct-1999. National Geological Society of America Meeting. Denver, CO, USA.

Chouinard, L.E., Bennett, D.W., Feknous, N., 1995. statistical analysis of monitoring data for concrete arch dams. J. Perform. Constr. Facil. 9 (November (4)), 286–301.

Colesanti, C., Ferretti, A., Novali, F., Prati, C., Rocca, F., 2003. SAR monitoring of progressive and seasonal ground deformation using the permanent scatterers technique. IEEE Trans. Geosci. Remote Sens. 41 (July (7)), 1685–1701.

De Sortis, A., Paoliani, P., 2007. Statistical analysis and structural identification in concrete dam monitoring. Eng. Struct. 29 (January (1)), 110–120.

De Sousa, J.J., Lazecky, M., Hlavacova, I., Bakon, M., Patricio, G., Perissin, D., 2015. Satellite SAR interferometry for monitoring dam deformations in Portugal. In: Second International Dam World Conference, Portugal, April 21–24, p. 2015.

Di Martire, D., Iglesias, R., Monells, D., Centolanza, G., Sica, S., Ramondini, M., Calcaterra, D., 2014. Comparison between differential SAR interferometry and ground measurements data in the displacement monitoring of the earth-dam of Conza della Campania (Italy). Remote Sens. Environ. 148, 58–69.

2014. ENI Report, http://www.eni.com/files/media/news/ENI%20Basilicata%20Relazione_evento28dic_2014_finale.pdf (last time accessed August 2015).

Ehiorobo, J.O., Irughe-Ehigiator, R., 2011. Monitoring for horizontal movement in an earth dam using differential GPS. J. Emerg. Trends Eng. Appl. Sci. 2 (6), 908–913.

Ferretti, A., Prati, C., Rocca, F., 2000. Nonlinear subsidence rate estimation using permanent scatterers in differential SAR interferometry. IEEE Trans. Geosci. Remote Sens. 38 (5), 2202–2212, http://dx.doi.org/10.1109/36.868878.

Ferretti, A., Prati, C., Rocca, F., 2001. Permanent scatterers in SAR interferometry. IEEE Trans. Geosci. Remote Sens. 39 (1), 8–20, http://dx.doi.org/10.1109/36.898661.

Giocoli, A., Stabile, T.A., Adurno, I., Perrone, A., Gallipoli, M.R., Gueguen, E., Piscitelli, S., 2014. Geological and geophysical characterization of the south-eastern side of the High Agri Valley (southern Apennines Italy). Nat. Hazards Earth Syst. Sci. Discuss. 2 (10), 6271–6294.

Giocoli, A., 2014. Evidence of low-magnitude continued reservoir-induced seismicity associated with the pertusillo artificial lake (Southern Italy). Bull. Seismol. Soc. Am.

Grenerczy, G., Wegmüller, U., 2011. Persistent scatterer interferometry analysis of the embankment failure of a red mud reservoir using ENVISAT ASAR data. Nat. Hazards 59, 1047–1053.

Léger, P., Leclerc, M., 2007. Hydrostatic, temperature, time-displacement model for concrete dams. J. Eng. Mech. 133 (3), 267–277.

Li, W., Wang, C., 2011. GPS in the tailings dam deformation monitoring. Procedia Eng. 26, 1648–1657.

Lombardi, G., Amberg, F., Darbre, G.R., 2008. Algorithm for the prediction of functional delays in the behaviour of concrete dams. Int. J. Hydropower Dams 15 (3), 111.

Lundgren, P., Kiryukhin, A., Milillo, P., Samsonov, S., 2015. Dike model for the 2012–2013 Tolbachik eruption constrained by satellite radar interferometry observations. J. Volcanol. Geotherm. Res. 307, 79–88.

Mazzanti, P., Perissin, D., Rocca, A., 2015. Structural health monitoring of dams by advanced satellite SAR interferometry: investigation of past processes and future monitoring perspectives. In: 7th Internation Conference on Structural Health Monitoring of Intelligent Infrastructure, Torino, Italy, July 1–3 2015.

Michoud, C., Baumann, V., Derron, M.H., Jaboyedoff, M., Lauknes, T.R., 2015a. Slope instability detection along the national 7 and the potrerillos dam reservoir, Argentina, using the small-baseline InSAR technique. Engineering Geology for Society and Territory, vol 2. Springer International Publishing, pp. 295–299.

Michoud, C., Baumann, V., Lauknes, T.R., Penna, I., Derron, M.H., Jaboyedoff, M., 2015b. Large slope deformations detection and monitoring along shores of the

Potrerillos dam reservoir, Argentina, based on a small-baseline InSAR approach. Landslides, 1–15.
Milillo, P., Fielding, E.J., Shulz, W.H., Delbridge, B., Burgmann, R., 2014. COSMO-SkyMed spotlight interferometry over rural areas: the Slumgullion landslide in Colorado, USA. IEEE J. Sel. Top. Appl. Earth Obs. Remote Sens. 7 (7), 2919–2926.
Milillo, P., Riel, B., Minchew, B., Yun, S.H., Simons, M., Lundgren, P., 2015. On the Synergistic Use of SAR Constellations' Data Exploitation for Earth Science and Natural Hazard Response.
Milillo, P., 2016. The synergistic use of synthetic aperture radar constellations for studying natural and anthropogenic phenomena. In: PhD Thesis in Environmental Enginering. University of Basilicata, Potenza, Italy.
Perissin, D., Prati, C., 2008. Identifying urban SAR permanent scatterers for motion interpretation and multi-track data fusion. Riv. ital. Telerilevamento 40 (2), 115–121.
Perissin, D., Prati, C., Rocca, F., 2007a. ASAR parallel-track PS analysis in urban sites. In: Geoscience and Remote Sensing Symposium, 2007, IGARSS 2007. IEEE International, pp. 1167–1170.
Perissin, D., Prati, C., Rocca, F., Li, D., Liao, M., 2007b. Multi-track PS analysis in Shanghai. Proc. ENVISAT 200, 23–32.
Perissin, D., Wang, Z., Wang, T., 2011. The SARPROZ InSAR tool for urban subsidence/manmade structure stability monitoring in China. In: 34th International Symposium for Remote Sensing of the Environment (ISRSE), Syndey, Australia (2011, January).
Perissin, D., 2008. Validation of the submetric accuracy of vertical positioning of PSs in C-band. Geosci. Remote Sens. Lett. IEEE 5 (3), 502–506.
Riel, B., Milillo, P., Simons, M., Lundgren, P., Kanamori, H., Samsonov, S., 2015. The collapse of BárÐarbunga caldera, Iceland. Geophys. J. Int. 202 (1), 446–453.
Roque, D., Perissin, D., Falcão, A.P., Fonseca, A.M., Henriques, M.J., Franco, J., 2015. Dams regional safety warning using time-series InSAR techniques. In: Second International Dam World Conference, Portugal, April, pp. 21–24.
Stabile, T.A., Giocoli, A., Lapenna, V., Perrone, A., Piscitelli, S., Telesca, L., 2014a. Evidence of low-magnitude continued reservoir-induced seismicity associated with the Pertusillo Artificial Lake (Southern Italy). Bull. Seismol. Soc. Am. 104 (4), 1820–1828.
Stabile, T.A., Giocoli, A., Perrone, A., Piscitelli, S., Lapenna, V., 2014b. Fluid injection induced seismicity reveals a NE dipping fault in the southeastern sector of the High Agri Valley (southern Italy). Geophys. Res. Lett. 41 (16), 5847–5854.
Tarchi, D., Rudolf, H., Luzi, G., Chiarantini, L., Coppo, P., Sieber, A.J., 2016. SAR in-terferometry for structural changes detection: a demonstration test on a dam. Hamburg, Germany In: Proceedings of the IEEE International Geoscience and Remote Sensing Symposium (IGARSS '99), vol. 3, pp. 1522–1524 (1999, July).
Tomás, R., Cano, M., Garcia-Barba, J., Vicente, F., Herrera, G., Lopez-Sanchez, J.M. et al., (2013, May 8). Monitoring an earthfill dam using differential SAR interferometry: La Pedrera Dam, Alicante, Spain. Engineering Geology, 157, Elsevier.
Vöge, M., Larsen, Y., Frauenfelder, R., 2011. Monitoring dams and reservoir slopes with interferometric SAR. In: Proc. 8th Intern. Symp. on Field Measurements in GeoMechanics, Berlin, Germany, September, pp. 12–16.
Wang, T., Perissin, D., Rocca, F., et al., 2010. Three Gorges Dam stability monitoring with time-series InSAR image analysis. Sci. China Earth Sci., http://dx.doi.org/10.1007/s11430-010-4101-1.